1D MOS Nanostructures

Subjects: Others

Contributor: Weronika Smok

1D electrospun MOS are basically nanofibers, nanotubes or nanowires, which are made of one or more semiconductor metal oxides or with other dopant material. Polymer/MOS precursor nanofibers that are formed in the electrospinning process are calcined until the polymer is removed and pristine MOS nanostructure is obtained.

electrospinning metal oxides nanomaterials nanofibers nanowires

1. Electrospun 1D MOS in Saving the Natural Environment

Industrialization and increasing consumerism have led to the highest level of warning about environmental pollution and its associated crisis. Industrial waste compared to municipal waste is toxic and non-biodegradable, as it contains heavy metal ions, oils and fats, dyes, phenols and ammonia, which can adversely affect human life and health but also the environment. One possible solution to this problem is to use the process of photocatalysis to break down harmful substances into simpler and environmentally friendly ones. Photocatalysis combines reactions using light and a catalyst, which is usually a semiconductor—it absorbs light and acts as a catalyst for chemical reactions. Therefore, it is necessary to search for semiconductor materials that can help solve this global problem.

Recently, electrospun one-dimensional semiconductor metal oxide nanostructures, predisposed by their unique optical and electrical properties, have attracted the attention of researchers studying photocatalytic pollutant decomposition processes of TiO_2, ZnO and SnO_2, whose energy gap width, radiation absorption range and mobility rate can be controlled by the parameters of the manufacturing process (**Figure 1**, **Table 1** and **Table 2**) [1][2][3][4][5][6].

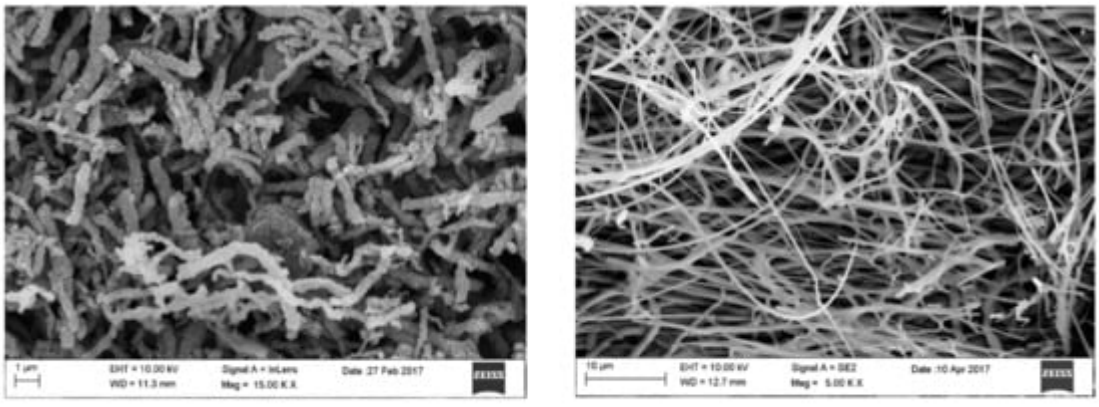

(a) (b)

Figure 1. SEM image of surface morphology of (**a**) TiO_2 nanowires after calcination at 400 °C, (**b**) ZnO nanowires after calcination at 400 °C [own study].

Table 1. Optical properties of selected 1D metal oxides prepared via electrospinning.

MOS	TiO_2	ZnO	SiO_2	SnO_2	Bi_2O_3	In_2O_3
Direct band gap [eV]	2.91–2.94	3.32–3.36	3.93–3.97	3.30–3.58	2.48–2.72	2.92–3.34
Ref.	[1]	[7]	[8]	[9]	[10]	[11][12]

Table 2. Optical properties of TiO_2 nanowires and ZnO nanowires after calcination at 400 °C [own study].

Material	Calcination Temperature [°C]	Max. Absorbance	Wavelength [nm]	Eg [eV]
TiO_2 nanowires	400	2.42	248	3.73
	500	2.34		3.83
	600	2.26		3.88
ZnO nanowires	400	2.94	346	3.36
	500	3.38		3.34
	600	3.43		3.32

Z. Wang et al. performed an analysis [13] of the photocatalytic properties of ZnO/SnO_2 nanofiber with and without the addition of the P123 precursor, which resulted in a much higher photocatalytic activity in the degradation of methyl orange (MO) in UV light of the composite nanofibers with the addition of P123. C. Zhu et al. in their work [14] showed significantly greater possibilities of photocatalytic decomposition of Rhodamine B in visible light through the use of composite SnO_2/Fe_2O_3 nanofibers compared to the capabilities of the non-admixture SnO_2. Electrospun SnO_2 nanostructures coated with a 1 nm thick carbon shell fabricated by P. Zhang et al. [15] showed very efficient photocatalytic degradation of 4-Nitrophenol under both UV and visible light (**Figure 2**). K. Wang et al. in their work [16] reported a study on the photocatalytic activity of mutiheterojunction in the photodegradation of methyl orange (MO) and Cr (VI) ions under visible light. It was observed that the SnO_2/Bi_2O_3/BiOI nanofibers were characterized by better photocatalytic activity than the non-admixture SnO_2 and Bi_2O_3, which the authors attributed to the increased absorption of visible light, electron-hole pair separation and large specific surface area of the nanostructures studied.

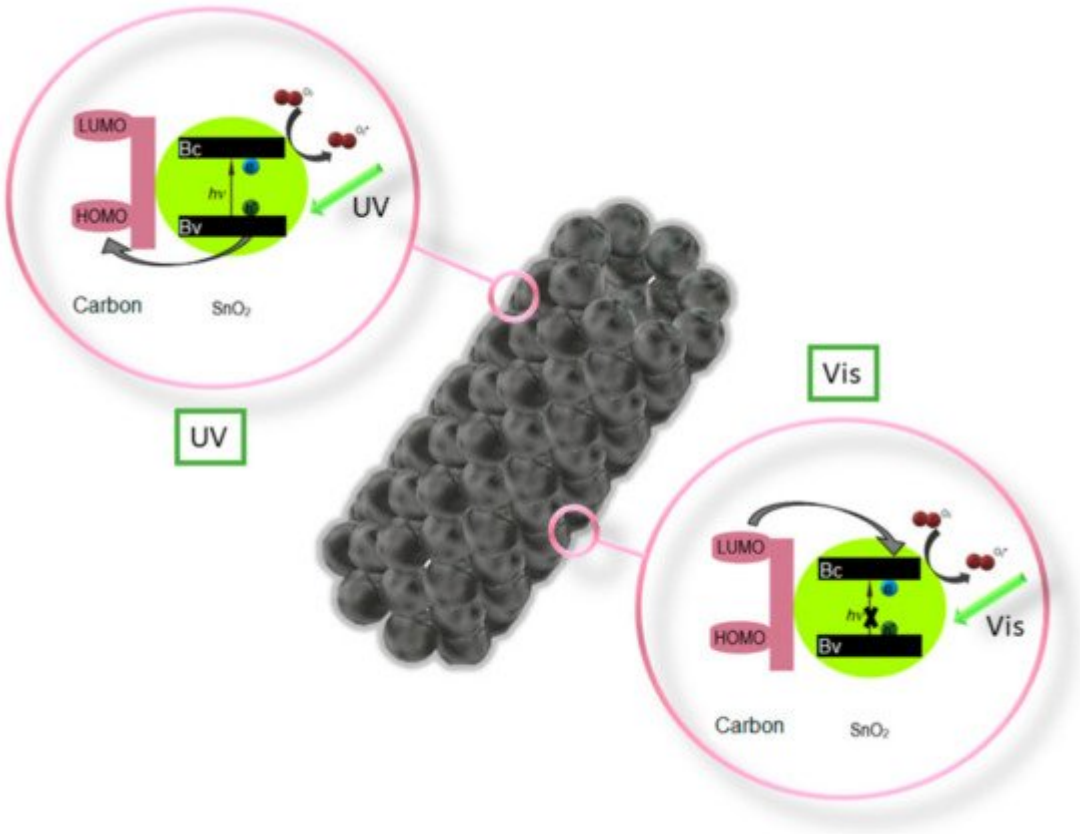

Figure 2. Diagram of the photocatalytic activation of nanotubes SnO_2 [15].

T. Wang. et al. [1] demonstrated that the use of magnetic field-assisted electrospinning in the fabrication of nanofibers and nanotubes from TiO_2 narrowed the band gap to favor photocatalytic performance—TiO_2 reduced Rhodamine B (RhB) by 95.8% in 100 min. Q. Zhang et al. [17] proposed the use of 1D composite nanostructures based on In_2O_3 of admixtured $CaIn_2O_4$ in the photocatalytic purification of water from the dye-methylene blue (MB). The degradation rates of MB were 76% and 92%, respectively, under 120 min of simulated sunlight exposure. The efficient separation and transport of photogenerated carriers, as well as the large specific surface area, meant that the $CaIn_2O_4$-In_2O_3 composites were characterized by high photocatalytic efficiency. A. Ahmad et al. [18] by the triaxial electrospinning method produced TiO_2 with a structure of nanofiber-in-nanotube (rutile-anatase), with which the photodegradation was carried out for 88.1% of the Sandalfix N. Blue with a 240 min irradiation time.

The diversity of available variations of the electrospinning process makes it possible to obtain MOS with high photocatalytic activity; however, further research is needed to explore the mechanism of this phenomenon.

The growing demand for green energy motivates researchers to look for materials and solutions that can increase the efficiency of existing renewable energy sources (RES), especially photovoltaic cells. So far, the many works that have presented the possibility of using 1D MOS in the construction of modern solar cells mainly focused on the use of TiO_2, ZnO and SnO_2 [19][20][21][22][23][24][25][26][27].

Favorable optoelectronic properties of crystalline-amorphous hybrid SnO_2 nanowires are suggested by W. Matysiak et al. [28] to be used in in modern flexible photovoltaic cells (**Table 3**, **Figure 3**). The research group, to which the Authors belong, was awarded a silver medal at the 5th China (Shanghai) International Invention & Innovation Expo in 2021 for the invention "Innovative flexible solid-state solar cell with a hybrid layered architecture", for which the construction of which SnO_2 nanowires were used (**Figure 4**).

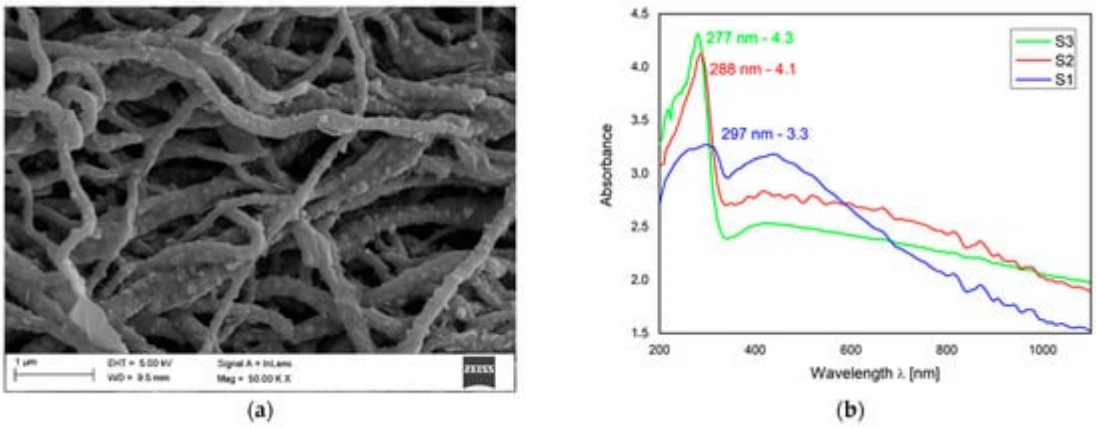

Figure 3. (**a**) SEM image of SnO_2 nanowires calcined in 500 °C (Reprinted with kind permission from Springer [28]); UV-VIS: (**b**) absorption spectrum of SnO_2 nanowires calcined in 500 °C (Reprinted with kind permission from Nature [29]).

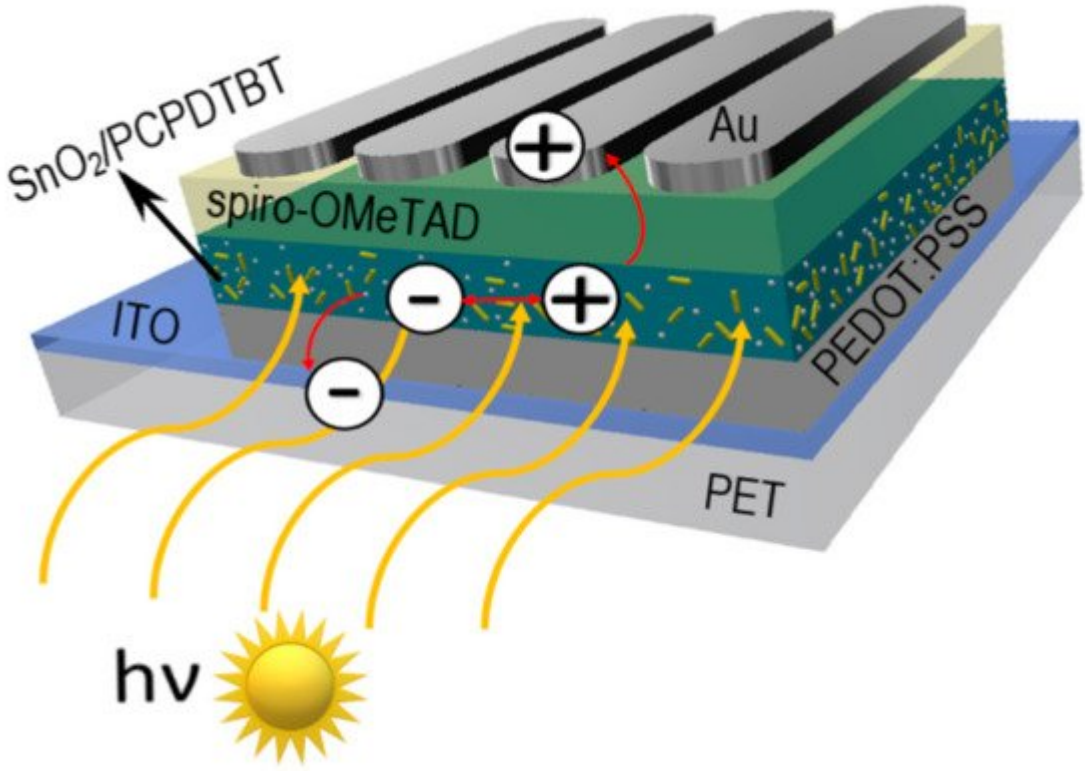

Figure 4. Schematic representation of multilayer flexible photovoltaic architecture manufactured in Department of Engineering Materials and Biomaterials [Poster at the 5th China (Shanghai) International Invention & Innovation Expo: "Innovative flexible solid-state solar cell with a hybrid layered architecture"].

Table 3. Refractive index and dielectric permittivity obtained for the electrospun 1D SnO_2 nanomaterials [28].

Parameter	SnO_2 Nanowires		
	Type of Spinning Solutions		
	Type 1	Type 2	Type 1
refractive index (n)	1.51	1.52	1.51
complex dielectric permeability (ε)	2.28	2.30	2.28
Energy band gap (E_g)	3.3	3.8	3.9

M. Yang et al. in their publication [30] described the effect of graphene oxide (GO) admixture in hybrid SnO_2/TiO_2 nanofibers on the efficiency of dye-based solar cells (DSCs) constructed with their participation. DSCs along with GO-SnO_2/TiO_2 as the working electrode were analyzed for efficiency and the following photovoltaic parameters: short-circuit current density, open-circuit voltage and fill factor, which were respectively 11.19 mA/cm^2, 0.72 V and 0.67. It was found that the solar-to-electric energy conversion efficiency of GO/SnO_2/TiO_2 as a photoanode-based device was 5.41%.

Therefore, it is worthwhile to pay attention to the application of MOS in the construction of next-generation photovoltaic cells, as they may provide a solution to the problem of low efficiency of dye-based cells.

2. Electrospun Metal Oxides 1D Nanostructures in Gas Sensors

The most widely studied application of one-dimensional metal oxide-based nanostructures are sensors for gases such as methanol, ethanol, acetone, formaldehyde, xylene and other volatile organic compounds that are highly toxic and dangerous to human health and even life [31][32].

Gas sensors based on semiconductor metal oxides are widely used in many areas, including chemical pollution control in air and rooms, alarms to detect the threat of poisonous substances and even medical diagnostics performed on the basis of a patient's breath. The popularity of these types of sensors is due to their high sensitivity, low cost and ease of manufacture, as well as their compatibility with modern electronic devices [33][34][35][36][37][38].

The mechanism of gas detection by these MOS can be explained by the fact that the conductivity of the materials is changed by the chemical interaction between the gas and the surface of the nanostructure on which oxygen is adsorbed. Oxygen (O_2) molecules are adsorbed on the nanofiber/nanowire surface in air and then they capture electrons from the conductivity band of the oxide so that chemisorbed oxygen ions (O_2^-) are generated and the formation of a barrier layer at a certain depth of the oxide structure is initiated. When the nanostructures are exposed to gas at an appropriate temperature, the gas reacts with the surface oxygen species and the width of the barrier layer decreases. As a result, the carrier concentration will increase, which ultimately increases the conductivity of the nanofibers/nanowires [39][40][41].

Many scientific reports indicate that the detection of hazardous substances by sensors based on electrospun MOS still needs to be developed—obtaining sensors with a lower substance detection threshold and shorter device response and reaction times. Improvement of these properties can be achieved by admixing with metallic nanoparticles, other MOS and carbon materials, which will affect the conductivity of the MOS. The combination of different materials produces local p-n, n-n or p-p nanojunctions. It is the heterojunctions generated from different materials that directly affect the substance detection mechanism. Several typical morphologies of MOS-based heterostructured materials are most commonly reported in the literature (**Figure 5**). In addition to non-admixed 1D MOS, hybrid structures consisting of both MOS and admixed crystallites simultaneously stand out. MOS nanowires decorated with nanoparticles or other forms of admixture are another interesting variation. There are also structures with core-shell morphology in which MOS can be either covered or surrounded by other material.

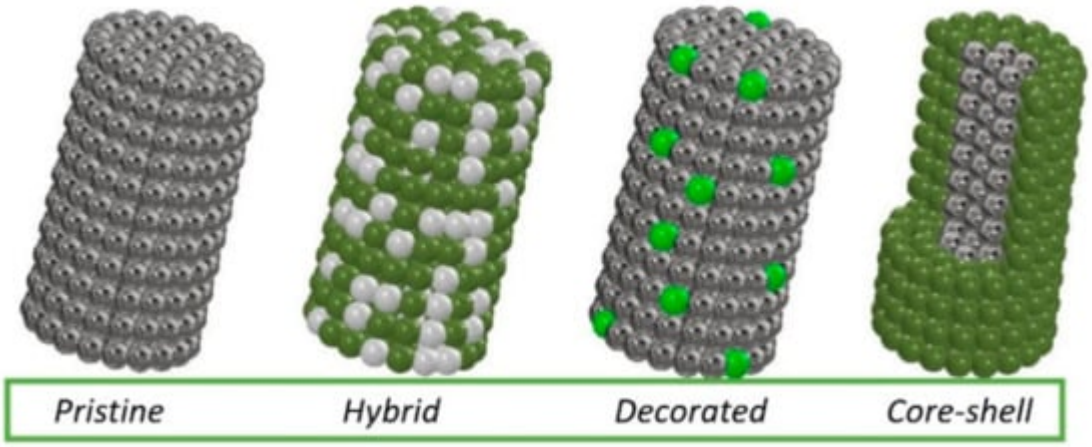

Figure 5. Types of morphology of the most commonly produced 1D nanostructures.

One of the most commonly used MOS as detector anode is tin dioxide, which is characterized by an energy gap width of about 3.6 kV and simultaneous optical transparency and electrical conductivity [40][42][43][44][45][46]. Indium oxide exhibiting similar properties to tin oxide is also increasingly used. These materials are often combined with each other and also admixed with other oxides such as TiO_2, ZnO, CuO and NiO (**Table 4**). The authors of this paper have established a collaboration with the Department of Optoelectronics, which is equipped with laboratories capable of gas detection measurements. Electrospun SnO_2 and In_2O_3 nanowires fabricated in the Department of Engineering Materials and Biomaterials will be plotted on the IDT and tested to detect gases such as NH_3, NO_2, CO_2 and H_2.

Bai et al. [47] demonstrated that the porous, coreless structure of ZnO-SnO_2 nanowires is ideal for detecting very low concentrations (0.023 ppm) of toxic NO_2. In addition, good detection properties of NO_2 promotes the formation of an n-n heterojunction at the phase boundary of ZnO and SnO_2, which results in the formation of an additional barrier layer (**Figure 6**).

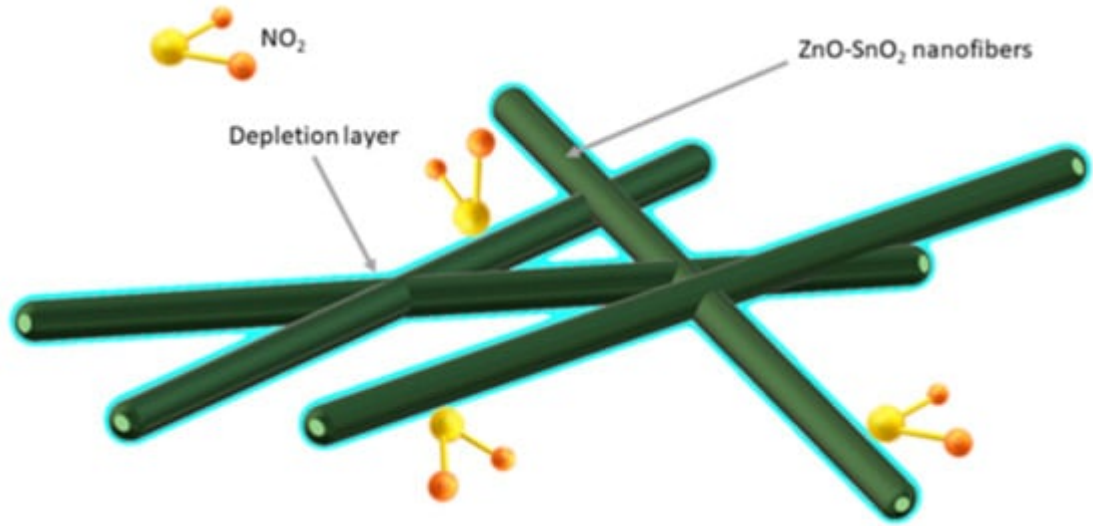

Figure 6. Scheme of hollow structure of gas adsorption and depletion layer for $ZnO\text{-}SnO_2$ composite [47].

Zhang et al. [48] observed that the response of sensors in acetone-containing environment can be improved by using heterojunction nanotubes of $WO_3\text{-}SnO_2$ and admixing it with Pd catalyst. Studies of the sensory properties of the material showed that the addition of Pd increased the response of $Pd\text{-}WO_3\text{-}SnO_2$ sensor more than double the response obtained from $WO_3\text{-}SnO_2$ sensor in contact with 100 ppm acetone. In addition, the selectivity for detecting acetone in the presence of other gases such as toluene, ammonia, nitrous oxide and pentane was significantly improved.

Du et al. [49] fabricated In_2O_3 nanofibers with a traditional electrospinning method and then they subjected them to surface modification using low-temperature oxygen and hydrogen radiofrequency plasma. The nanofibers were placed in a plasma reactor chamber and surface modification was performed by increasing the number of pores and channels in the nanofibers (**Figure 7**). This mechanism enabled more oxygen to be adsorbed on the surface of the indium oxide nanostructures, leading to increased response values and improved selectivity for detecting acetone in the presence of interfering gases such as ethanol, methanol, formaldehyde, benzene, ammonia and nitrogen dioxide.

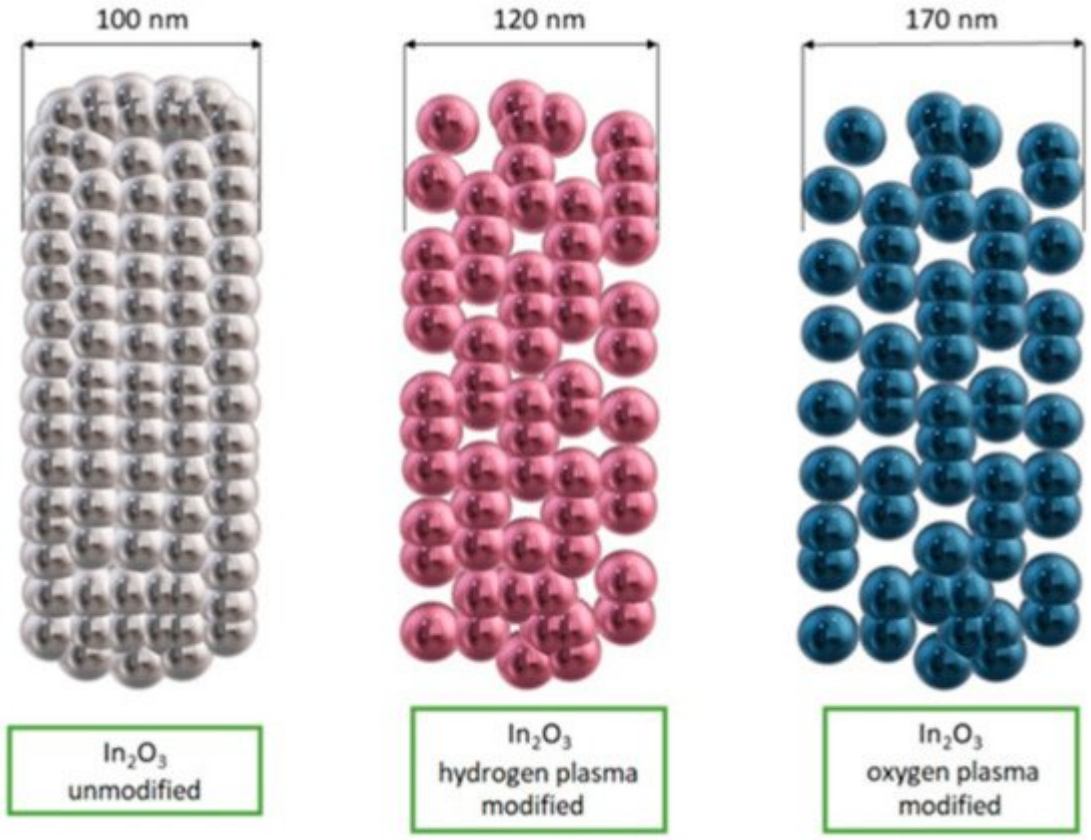

Figure 7. Scheme of In_2O_3 nanofibers morphology before and after surface modification [49].

Table 4. Selected 1D MOS and their sensing properties.

Material Type	Polymer	Precursor	Solvent	Calcination Time [h]	Calcination Temp [°C]	Gas	Conc [ppm]	Response/Recovery Time [s]	Ref.
ZnO-SnO_2	PVP	$SnCl_2{\cdot}2H_2O$, $Zn(AC)_2{\cdot}2H_2O$	DMF, EtOH	3	600	Toluene	1-300	6–11/12–23	[50]
NiO-SnO_2	PVP	$SnCl_2{\cdot}2H_2O$, $NiCl_2{\cdot}6H_2O$	DMF, EtOH	5	600	Toluene	50	11.2/4	[51]
CuO-SnO_2	PVA	$SnCl_2{\cdot}2H_2O$, $CuCl_2{\cdot}2H_2O$	DMF, EtOH	4	600	H_2S	10	1/10	[52]
CeO_2-SnO_2	PVP	$SnCl_2{\cdot}2H_2O$, $Ce(NO_3)_3{\cdot}6H_2O$	DMF, EtOH	3	600	EtOH	200	8–10/11–30	[53]
W_2O_3-SnO_2	PVP	$SnCl_2{\cdot}2H_2O$/ $(NH_4)_6H_2W_{12}O_{40}{\cdot}xH_2O$	DMF, EtOH	1	600	EtOH	10	18.5/282	[54]
Fe_2O_3-In_2O_3	PVP	$In(NO_3)_3{\cdot}4.5H_2O$, $Fe(NO_3)_3{\cdot}9H_2O$	DMF, EtOH	2	550	Formaldehyde	100	5/25	[55]

Material Type	Polymer	Precursor	Solvent	Calcination Time [h]	Calcination Temp [°C]	Gas	Conc [ppm]	Response/Recovery Time [s]	Ref.
WO_3-In_2O_3	PVP	$In(NO_3)_3{\cdot}4.5H_2O$, WCl_6	DMF, EtOH, AcOH	2	500	Acetone	25	6/64	[56]
CuO-In_2O_3	PVP	$In(NO_3)_3{\cdot}xH_2O$, $Cu(NO_3)_2{\cdot}xH_2O$	DMF	2	600	H_2S	5	4–30/incomplete recovery	[57]
SnO_2-In_2O_3	PVP	$In(NO_3)_3{\cdot}4.5H_2O$, $SnCl_2{\cdot}2H_2O$	DMF, EtOH	2	600	Formaldehyde	0.5-50	~20/40	[58]
In_2O_3 (RF plasma modified)	PVP	$In(NO_3)_3{\cdot}4.5H_2O$	DMF, EtOH	3	550	Acetone	10	18–23/55–92	[49]
La_2O_3-In_2O_3	PVP	$In(NO_3)_3{\cdot}xH_2O$, $La(NO_3)_3{\cdot}xH_2O$	DMF, EtOH, mineral oil	2	550	Formaldehyde	50	3/19	[59]
In_2O_3	PVP	$In(NO_3)_3{\cdot}4.5\ H_2O$	DMF	2	800	NO_2	5	200/1000	[60]

uction of
posed to

3. Electrospun Metal Oxides 1D Nanostructures in Other Applications

Supercapacitors and lithium-ion batteries (LIBs) are other devices for which one-dimensional MOS nanostructures can be used. With the rapid progress of civilization and industrialization, there is a growing need for methods, materials and devices to store large amounts of energy [61]. One solution to meet these needs is the development of LIBs with high performance, which is primarily dependent on the performance of the battery's most important component, the anode. The currently used anode material in the form of graphite is currently no longer able to meet the needs of high energy storage capacity due to its low capacity and low efficiency. Therefore, the search and research of new electrode materials is of great importance for the current demand for high performance LIBs [62][63]. Recently, semiconductor nanomaterials such as ZnO, NiO, SnO_2 lub TiO_2 nanotubes and nanowires have been of particular interest for 1D, along with heterojunctions formed by combining these materials with carbon materials [64][65][66][67][68][69]. The advantage of using one-dimensional nanomaterials for anodes in LIBs is the much less frequently observed agglomeration of the material than in the case of nanoparticles, which positively affects the electrochemical performance of the battery, and this fact was confirmed in a study by C. K. Chan et al. [70] based on the analysis of a battery based on Si nanowires.

J. Zhu et al. [68] pointed out the high application potential of electrospun ZnO-SnO_2 nanofibers as anode material in lithium-ion batteries. It was observed that due to the heterogeneous mesoporous electrode structure based on ZnO-SnO_2 nanofibers, they provide excellent performance and reversible capacity at a relatively low cost and with high process repeatability. D. Lei et al. in their work [71] showed that GeO_2-SnO_2 composite nanofibers with high porosity prepared by the solution electrospinning method have high specific capacitance and good cycling performance, which is mainly due to the porous one-dimensional nanostructure, which can shorten the transport pathway and provide trapping of electrolyte ions to meet the requirements of fast charging and discharging

reactions. J. Guo in [72] described the effect of pore distribution on the capacitance of two types of porous C/SnO_2 nanofibers produced by electrospinning from solutions based on different precursors, i.e., using tin chloride, the fibers with spherical pores were obtained, while the pores in the form of channels were obtained from acetate (**Figure 8**). On the basis of a galvanostatic charge-discharge test, it was found that multichannel C/SnO_2 nanofibers with a large specific surface area (34.97 m^2/g) achieve better charging performance than spherical pore nanofibers and show a more stable capacity retention of about 90% after 50 cycles.

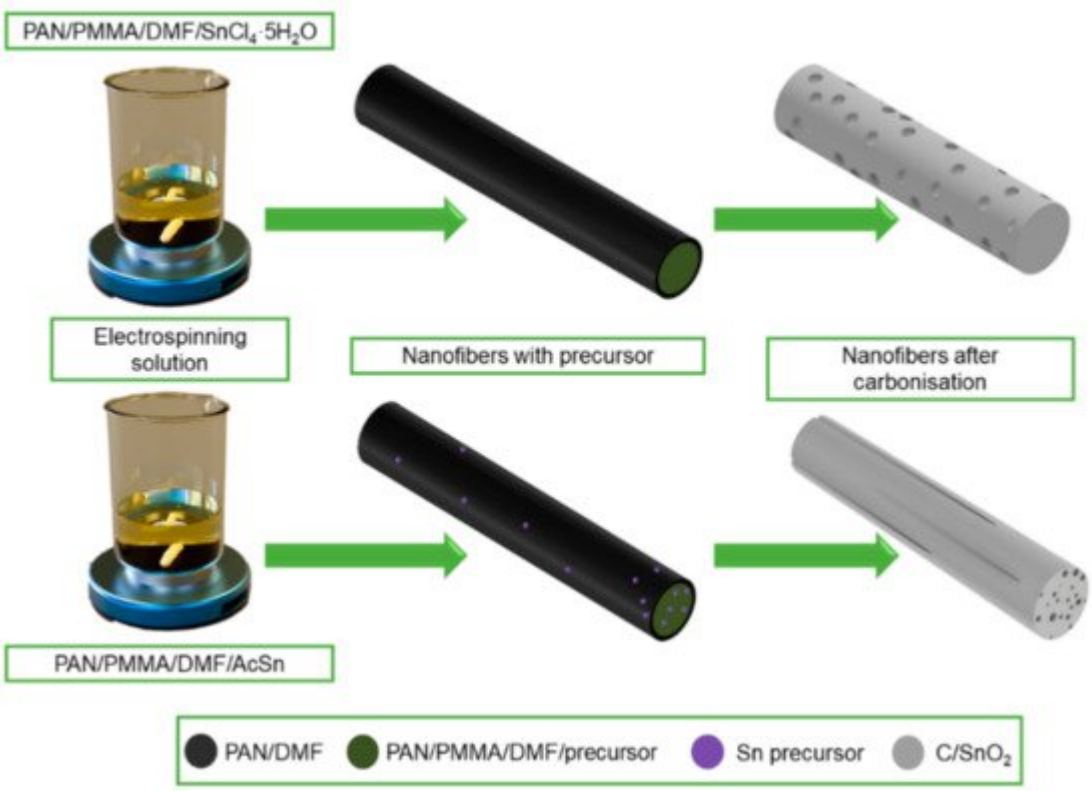

Figure 8. Scheme of the manufacturing process of C/SnO_2 nanofibers with a different morphology.

The use of SnO_2-ZnO nanofibers in energy storage was presented in the work [69] of J. Zhang et al. The study showed that by using the spinning solution parameters, it is possible to control the morphology and obtain hollow nanotubes, which exhibited good capacity stability in an electrochemical test. In addition, it was observed that the polypyrrole (PPy) polymer coating of SnO_2-ZnO nanotubes has made it possible to maintain a high capacity of 626.1 mA hg^{-1} at 0.2 °C for 100 cycles, and cycle stability has also been improved.

Thus, the electrospinning method with subsequent calcination enables precise control of the electrochemical properties of the fabricated one-dimensional MOS-based nanostructures, thus providing a chance to solve the problem of non-compliant LIBs.

Due to their unique optical, electrical and magnetic properties, they are used in modern devices such as field-effect transistors (FETs) and microwave absorption materials. X. Zhu et al. presented [73] a method to fabricate high-performance field-effect transistors based on electrospun In_2O_3 nanofibers admixed with Al, Ga and Cr. The devices showed optimal performance at a 10% molar concentration of admixing material (Al, Cr and Ga): low and

positive gate-source voltage V_{GS} (<6.0 V), a high ratio of the transistor on current to transistor off current I_{on}/I_{off} (~108), high saturation current (~10–4 A) and carrier mobility on the level of ~2.0 $cm^2/V^{-1}s^{-1}$.

H. Zhang et al. [13] demonstrated that the use of polymorphic anatase-rutile TiO_2 nanofibers to build FET showed better transistor characteristics because of a strong synergistic effect compared with pure anatase and rutile TiO_2 nanofibers. BioFET created by S. Veeralingam and S. Badhulik [74] based on β–Bi_2O_3 nanofibers for the detection of serotonin exhibited sensitivity of 51.64 µA/nM over a range of 10 nM^{-1} µM and a limit of detection of 0.29 nM. Moreover, it maintained excellent sensitivity, stability and reproducibility with a rapid response time of 0.8 s. Using the electrospinning method, K.C.S. Reddy et al. [75] created a self-powered NiO-p/Si-n based ultraviolet photodetector which exhibited a high responsivity of 9.1 mA W^{-1} at zero bias with a fast photoresponse of less than 0.4 s. X. Huang et al. [76] observed that electrospun bead-like Co-ZnO nanostructures present ferromagnetic properties and an excellent electromagnetic loss performance—the effective microwave absorption of bandwidth with reflection loss less than −10 dB was 11.6 GHz.

For years, medicine has been a priority discipline in which new solutions and biomaterials are constantly being sought. Looking at the disease problems that affect mankind today, the most rapidly developing areas of medicine include cancer therapies, drug delivery, biosensors, medical imaging and tissue engineering. Due to the unsatisfactory properties of conventional biomaterials, it is necessary to search for new material solutions. Production of one-dimensional nanomaterials with controlled dimensions, arrangement of structures with respect to each other or porosity creates many possibilities of using their unique properties for therapeutic purposes. Ceramic nanomaterials, which are based on inert simple oxides, may seem to be a possible solution for some health problems. The most commonly used one-dimensional MOS include TiO_2, due to its non-toxicity, environmental friendliness as well as good chemical stability and high corrosion resistance [77][78].

One of many interesting examples of work on the above issue is that presented by I.H.M. Aly et al. [79], who used electrospun TiO_2 nanofibers as an admixture to a bioceramic composite based on wollastonite for bone tissue regeneration, which significantly improved the mechanical properties of the composite while not affecting the bioactivity in any way, and proves that this type of material is worth considering and researching for applications in medicine. Mesh with TiO_2 nanofibers may also find applications in tissue engineering, as studies have shown that it provides an osteogenic environment—increasing osteoblast production and differentiation [80]. S. Chen et al. confirmed the possibility of using hydrothermal treated nanofibers as delivery systems for the antibiotic tetracycline hydrochloride, whereby nanofibers showed high bactericidal activity against *E. coli* and *S. aureus* [81]. N.C. Bezir et al. demonstrated that TiO_2 and Ag/TiO_2 nanofibers show beneficial antibacterial properties based on measured inhibition zones diameters of *S. aureus*culture plates [82]. Effective inhibition of *B. subtilis* and *B. cereus* through TiO_2/GO/CA nanofibers was observed by L. Jia et al. [83]. TiO_2 in the form of electrospun one-dimensional nanostructures also shows promising results in promoting apoptosis of cancer cells, e.g., cervical cancer [84]. Other applications of 1D ceramic nanomaterials in medicine include the use of oleic acid-coated ZnO nanowires to fabricate hydrophobic polyvinylidene fluoride (PVDF) membranes, whose self-cleaning properties can be used to construct surgical devices and instruments or artificial blood vessels [85]. ZnO nanofibers, similarly to TiO_2 nanofibers, are characterized by tremendous antibacterial activity in *S. aureus and E. coli* utilization [86][87].

References

1. Wang, T.; Gao, Y.; Tang, T.; Bian, H.; Zhang, Z.; Xu, J.; Xiao, H.; Chu, X. Preparation of ordered TiO2 nanofibers/nanotubes by magnetic field assisted electrospinning and the study of their photocatalytic properties. Ceram. Int. 2019, 45, 14404–14410.
2. Zhang, J.; Hou, X.; Pang, Z.; Cai, Y.; Zhou, H.; Lv, P.; Wei, Q. Fabrication of hierarchical TiO2 nanofibers by microemulsion electrospinning for photocatalysis applications. Ceram. Int. 2017, 43, 15911–15917.
3. Nasr, M.; Balme, S.; Eid, C.; Habchi, R.; Miele, P.; Bechelany, M. Enhanced visible-light photocatalytic performance of electrospun rGO/TiO2 composite nanofibers. J. Phys. Chem. C 2017, 121, 261–269.
4. Boyadjiev, S.I.; Kéri, O.; Bárdos, P.; Firkala, T.; Gáber, F.; Nagy, Z.K.; Baji, Z.; Takács, M.; Szilágyi, I.M. TiO2/ZnO and ZnO/TiO2 core/shell nanofibers prepared by electrospinning and atomic layer deposition for photocatalysis and gas sensing. Appl. Surf. Sci. 2017, 424, 190–197.
5. Dursun, S.; Koyuncu, S.N.; Kaya, İ.C.; Kaya, G.G.; Kalem, V.; Akyildiz, H. Production of CuO–WO3 hybrids and their dye removal capacity/performance from wastewater by adsorption/photocatalysis. J. Water Process. Eng. 2020, 36, 101390.
6. Soares, L.; Alves, A. Photocatalytic properties of TiO2 and TiO2/WO3 films applied as semiconductors in heterogeneous photocatalysis. Mater. Lett. 2018, 211, 339–342.
7. Matysiak, W.; Tański, T.; Zaborowska, M. Manufacturing process, characterization and optical investigation of amorphous 1D zinc oxide nanostructures. Appl. Surf. Sci. 2018, 442, 382–389.
8. Matysiak, W.; Tański, T. Analysis of the morphology, structure and optical properties of 1D SiO2 nanostructures obtained with sol-gel and electrospinning methods. Appl. Surf. Sci. 2019, 489, 34–43.
9. Ch, S.R.; Zhang, L.; Kang, T.; Lin, Y.; Qiu, Y.; Reddy, A.S. Annealing impact on the structural and optical properties of electrospun SnO2 nanofibers for TCOs. Ceram. Int. 2018, 44, 4586–4591.
10. Lim, G.-D.; Yoo, J.-H.; Ji, M.; Lee, Y.-I. Visible light driven photocatalytic degradation enhanced by α/β phase heterojunctions on electrospun Bi2O3 nanofibers. J. Alloy. Compd. 2019, 806, 1060–1067.
11. Liu, W.; Xie, Y.; Chen, T.; Lu, Q.; Ur Rehman, S.; Zhu, L. Rationally designed mesoporous In2O3 nanofibers functionalized Pt catalysts for high-performance acetone gas sensors. Sens. Actuators B Chem. 2019, 298, 126871.

12. Lu, N.; Shao, C.; Li, X.; Miao, F.; Wang, K.; Liu, Y. A facile fabrication of nitrogen-doped electrospun In2O3 nanofibers with improved visible-light photocatalytic activity. Appl. Surf. Sci. 2017, 391, 668–676.
13. Wang, Z.; Li, Z.; Zhang, H.; Wang, C. Improved photocatalytic activity of mesoporous ZnO-SnO2 coupled nanofibers. Catal. Commun. 2009, 11, 257–260.
14. Zhu, C.; Li, Y.; Su, Q.; Lu, B.; Pan, J.; Zhang, J.; Xie, E.; Lan, W. Electrospinning direct preparation of SnO2/Fe2O3 heterojunction nanotubes as an efficient visible-light photocatalyst. J. Alloy. Compd. 2013, 575, 333–338.
15. Zhang, P.; Wang, L.; Zhang, X.; Shao, C.; Hu, J.; Shao, G. SnO2-core carbon-shell composite nanotubes with enhanced photocurrent and photocatalytic performance. Appl. Catal. B Environ. 2015, 166–167, 193–201.
16. Wang, K.; Qian, Z.; Guo, W. Multi-heterojunction of SnO2/Bi2O3/BiOI nanofibers: Facile fabrication with enhanced visible-light photocatalytic performance. Mater. Res. Bull. 2019, 111, 202–211.
17. Zhang, Q.; Cheah, P.; Han, F.; Dai, Q.; Yan, Y.; Pramanik, A.; Chandra Ray, P. Effects of calcination temperature on crystal structure and photocatalytic activity of CaIn2O4/In2O3 composites. Ceram. Int. 2019, 45, 21851–21857.
18. Ahmad, A.; Khan, M.A.; Nazir, A.; Arshad, S.N.; Qadir, M.B.; Khaliq, Z.; Khan, Z.S.; Satti, A.N.; Mushtaq, B.; Shahzad, A. Triaxial electrospun mixed-phased TiO2 nanofiber-in-nanotube structure with enhanced photocatalytic activity. Miroporous Mesoporous Mater. 2021, 320, 111104.
19. Mansouri, S.; Abbaspour-Fard, M.H.; Meshkini, A. Lily (Iris Persica) pigments as new sensitizer and TiO2 nanofibers as photoanode electrode in dye sensitized solar cells. Optik 2020, 202, 163710.
20. Li, X.; Gao, C.; Wang, J.; Lu, B.; Chen, W.; Song, J.; Zhang, S.; Zhang, Z.; Pan, X.; Xie, E. TiO 2 films with rich bulk oxygen vacancies prepared by electrospinning for dye-sensitized solar cells. J. Power Sources 2012, 214, 244–250.
21. Anjusree, G.S.; Deepak, T.G.; Nair, S.V.; Nair, A.S. Facile fabrication of TiO2 nanoparticle-TiO2 nanofiber composites by co-electrospinning-electrospraying for dye-sensitized solar cells. J. Energy Chem. 2015, 24, 762–769.
22. Mahmood, K.; Khalid, A.; Ahmad, S.W.; Mehran, M.T. Indium-doped ZnO mesoporous nanofibers as efficient electron transporting materials for perovskite solar cells. Surf. Coat. Technol. 2018, 352, 231–237.
23. Dinesh, V.P.; Sriram kumar, R.; Sukhananazerin, A.; Mary Sneha, J.; Manoj Kumar, P.; Biji, P. Novel stainless steel based, eco-friendly dye-sensitized solar cells using electrospun porous ZnO

nanofibers. Nano-Struct. Nano-Objects 2019, 19, 100311.

24. Mohamed, I.M.A.; Dao, V.-D.; Yasin, A.S.; Choi, H.-S.; Barakat, N.A.M. Synthesis of novel SnO2@TiO2 nanofibers as an efficient photoanode of dye-sensitized solar cells. Int. J. Hydrogen Energy 2016, 41, 10578–10589.
25. Bakr, Z.H.; Wali, Q.; Ismail, J.; Elumalai, N.K.; Uddin, A.; Jose, R. Synergistic combination of electronic and electrical properties of SnO2 and TiO2 in a single SnO2-TiO2 composite nanofiber for dye-sensitized solar cells. Electrochim. Acta 2018, 263, 524–532.
26. Lim, J.M.; Moon, J.; Kim, J.H.; Lee, C.O.; Chi, W.S.; Park, J.T. One-dimensional SnO2 nanotube solid-state electrolyte for fast electron transport and high light harvesting in solar energy conversion. Solid State Ionics 2021, 363, 115584.
27. Wei, K.; Gu, X.Y.; Chen, E.Z.; Wang, Y.Q.; Dai, Z.; Zhu, Z.R.; Kang, S.Q.; Wang, A.C.; Gao, X.P.; Sun, G.Z.; et al. Dissymmetric interface design of SnO2/TiO2 side-by-side bi-component nanofibers as photoanodes for dye sensitized solar cells: Facilitated electron transport and enhanced carrier separation. J. Colloid Interface Sci. 2021, 583, 24–32.
28. Matysiak, W.; Tański, T.; Smok, W. Study of optical and dielectric constants of hybrid SnO2 electrospun nanostructures. Appl. Phys. A Mater. Sci. Process. 2020, 126, 115.
29. Matysiak, W.; Tański, T.; Smok, W.; Polischuk, O. Synthesis of hybrid amorphous/crystalline SnO2 1D nanostructures: Investigation of structure, morphology and optical properties. Sci. Rep. 2020, 10, 14802.
30. Yang, M.; Li, X.; Yan, B.; Fan, L.; Yu, Z.; Li, D. Reduced graphene oxide decorated porous SnO2 nanotubes with enhanced sodium storage. J. Alloy. Compd. 2017, 710, 323–330.
31. Kim, J.-H.; Lee, J.-H.; Kim, J.-Y.; Mirzaei, A.; Kim, H.W.; Kim, S.S. Enhancement of CO and NO2 sensing in n-SnO2-p-Cu2O core-shell nanofibers by shell optimization. J. Hazard. Mater. 2019, 376, 68–82.
32. Wang, Q.; Bai, J.; Huang, B.; Hu, Q.; Cheng, X.; Li, J.; Xie, E.; Wang, Y.; Pan, X. Design of NiCo2O4@SnO2 heterostructure nanofiber and their low temperature ethanol sensing properties. J. Alloy. Compd. 2019, 791, 1025–1032.
33. Righettoni, M.; Amann, A.; Pratsinis, S.E. Breath analysis by nanostructured metal oxides as chemo-resistive gas sensors. Mater. Today 2015, 18, 163–171.
34. Güntner, A.T.; Pineau, N.J.; Mochalski, P.; Wiesenhofer, H.; Agapiou, A.; Mayhew, C.A.; Pratsinis, S.E. Sniffing entrapped humans with sensor arrays. Anal. Chem. 2018, 90, 4940–4945.
35. Tai, H.; Wang, S.; Duan, Z.; Jiang, Y. Evolution of breath analysis based on humidity and gas sensors: Potential and challenges. Sens. Actuators B Chem. 2020, 318, 128104.

36. Bhati, V.S.; Hojamberdiev, M.; Kumar, M. Enhanced sensing performance of ZnO nanostructures-based gas sensors: A review. Energy Rep. 2020, 6, 46–62.
37. Al-Hashem, M.; Akbar, S.; Morris, P. Role of oxygen vacancies in nanostructured metal-oxide gas sensors: A review. Sens. Actuators B Chem. 2019, 301, 126845.
38. Zhang, B.; Gao, P.-X. Metal oxide nanoarrays for chemical sensing: A review of fabrication methods, sensing modes, and their inter-correlations. Front. Mater. 2019, 6, 55.
39. Choi, J.-K.; Hwang, I.-S.; Kim, S.J.; Park, J.-S.; Park, S.-S.; Jeong, U.; Kang, Y.C.; Lee, J.-H. Design of selective gas sensors using electrospun Pd-doped SnO2 hollow nanofibers. Sens. Actuators B Chem. 2010, 150, 191–199.
40. Xu, S.; Kan, K.; Yang, Y.; Jiang, C.; Gao, J.; Jing, L.; Shen, P.; Li, L.; Shi, K. Enhanced NH3 gas sensing performance based on electrospun alkaline-earth metals composited SnO2 nanofibers. J. Alloy. Compd. 2015, 618, 240–247.
41. Wang, J.; Zou, B.; Ruan, S.; Zhao, J.; Chen, Q.; Wu, F. HCHO sensing properties of Ag-doped In2O3 nanofibers synthesized by electrospinning. Mater. Lett. 2009, 63, 1750–1753.
42. Wang, B.J.; Ma, S.Y. High response ethanol gas sensor based on orthorhombic and tetragonal SnO2. Vacuum 2020, 177, 109428.
43. Zhao, C.; Gong, H.; Niu, G.; Wang, F. Ultrasensitive SO2 sensor for sub-ppm detection using Cu-doped SnO2 nanosheet arrays directly grown on chip. Sens. Actuators B Chem. 2020, 324, 128745.
44. Onkar, S.G.; Raghuwanshi, F.C.; Patil, D.R.; Krishnakumar, T. Synthesis, characterization and gas sensing study of SnO2 thick film sensor towards H2S, NH3, LPG and CO2. Mater. Today 2020, 23, 190–201.
45. Li, N.; Fan, Y.; Shi, Y.; Xiang, Q.; Wang, X.; Xu, J. A low temperature formaldehyde gas sensor based on hierarchical SnO/SnO2 nano-flowers assembled from ultrathin nanosheets: Synthesis, sensing performance and mechanism. Sens. Actuators B Chem. 2019, 294, 106–115.
46. Das, S.; Jayaraman, V. SnO2: A comprehensive review on structures and gas sensors. Prog. Mater. Sci. 2014, 66, 112–255.
47. Bai, S.; Fu, H.; Zhao, Y.; Tian, K.; Luo, R.; Li, D.; Chen, A. On the construction of hollow nanofibers of ZnO-SnO2 heterojunctions to enhance the NO2 sensing properties. Sens. Actuators B Chem. 2018, 266, 692–702.
48. Zhang, J.; Zhang, L.; Leng, D.; Ma, F.; Zhang, Z.; Zhang, Y.; Wang, W.; Liang, Q.; Gao, J.; Lu, H. Nanoscale Pd catalysts decorated WO3–SnO2 heterojunction nanotubes for highly sensitive and selective acetone sensing. Sens. Actuators B Chem. 2020, 306, 127575.

49. Du, H.; Wang, H.; Yao, P.; Wang, J.; Sun, Y. In2O3 nanofibers surface modified by low-temperature RF plasma and their gas sensing properties. Mater. Chem. Phys. 2018, 215, 316–326.
50. Wei, S.; Zhang, Y.; Zhou, M. Toluene sensing properties of SnO2ZnO hollow nanofibers fabricated from single capillary electrospinning. Solid State Commun. 2011, 151, 895–899.
51. Liu, L.; Zhang, Y.; Wang, G.; Li, S.; Wang, L.; Han, Y.; Jiang, X.; Wei, A. High toluene sensing properties of NiO-SnO2 composite nanofiber sensors operating at 330 °C. Sens. Actuators B Chem. 2011, 160, 448–454.
52. Choi, S.-W.; Zhang, J.; Akash, K.; Kim, S.S. H2S sensing performance of electrospun CuO-loaded SnO2 nanofibers. Sens. Actuators B Chem. 2012, 169, 54–60.
53. Qin, W.; Xu, L.; Song, J.; Xing, R.; Song, H. Highly enhanced gas sensing properties of porous SnO2-CeO2 composite nanofibers prepared by electrospinning. Sens. Actuators B Chem. 2013, 185, 231–237.
54. Li, F.; Gao, X.; Wang, R.; Zhang, T. Design of WO3-SnO2 core-shell nanofibers and their enhanced gas sensing performance based on different work function. Appl. Surf. Sci. 2018, 442, 30–37.
55. Chi, X.; Liu, C.; Liu, L.; Li, S.; Li, H.; Zhang, X.; Bo, X.; Shan, H. Enhanced formaldehyde-sensing properties of mixed Fe2O3-In2O3 nanotubes. Mater. Sci. Semicond. Process. 2014, 18, 160–164.
56. Feng, C.; Li, X.; Ma, J.; Sun, Y.; Wang, C.; Sun, P.; Zheng, J.; Lu, G. Facile synthesis and gas sensing properties of In2O3-WO3 heterojunction nanofibers. Sens. Actuators B Chem. 2015, 209, 622–629.
57. Liang, X.; Kim, T.-H.; Yoon, J.-W.; Kwak, C.-H.; Lee, J.-H. Ultrasensitive and ultraselective detection of H2S using electrospun CuO-loaded In2O3 nanofiber sensors assisted by pulse heating. Sens. Actuators B Chem. 2015, 209, 934–942.
58. Du, H.; Wang, J.; Sun, Y.; Yao, P.; Li, X.; Yu, N. Investigation of gas sensing properties of SnO2/In2O3 composite hetero-nanofibers treated by oxygen plasma. Sens. Actuators B Chem. 2015, 206, 753–763.
59. Zeng, X.; Liu, L.; Lv, Y.; Zhao, B.; Ju, X.; Xu, S.; Zhang, J.; Tian, C.; Sun, D.; Tang, X. Ultra-sensitive and fast response formaldehyde sensor based on La2O3-In2O3 beaded nanotubes at low temperature. Chem. Phys. Lett. 2020, 746, 137289.
60. Zhang, B.; Bao, N.; Wang, T.; Xu, Y.; Dong, Y.; Ni, Y.; Yu, P.; Wei, Q.; Wang, J.; Guo, L.; et al. High-performance room temperature NO2 gas sensor based on visible light irradiated In2O3 nanowires. J. Alloy. Compd. 2021, 867, 159076.

61. Li, X.; Wang, J. One-dimensional and two-dimensional synergized nanostructures for high-performing energy storage and conversion. InfoMat 2020, 2, 3–32.
62. Song, B.; Loya, P.; Shen, L.; Sui, C.; He, L.; Guo, H.; Guo, W.; Rodrigues, M.-T.F.; Dong, P.; Wang, C.; et al. Quantitative in situ fracture testing of tin oxide nanowires for lithium ion battery applications. Nano Energy 2018, 53, 277–285.
63. Schiavi, P.G.; Farina, L.; Zanoni, R.; Altimari, P.; Cojocariu, I.; Rubino, A.; Navarra, M.A.; Panero, S.; Pagnanelli, F. Electrochemical synthesis of nanowire anodes from spent lithium ion batteries. Electrochim. Acta 2019, 319, 481–489.
64. Wang, W.; Liang, Y.; Kang, Y.; Liu, L.; Xu, Z.; Tian, X.; Mai, W.; Fu, H.; Lv, H.; Teng, K.; et al. Carbon-coated SnO2@carbon nanofibers produced by electrospinning-electrospraying method for anode materials of lithium-ion batteries. Mater. Chem. Phys. 2019, 223, 762–770.
65. Xia, J.; Zhang, X.; Yang, Y.; Wang, X.; Yao, J. Electrospinning fabrication of flexible, foldable, and twistable Sb2S3/TiO2/C nanofiber anode for lithium ion batteries. Chem. Eng. J. 2021, 413, 127400.
66. Oh, J.H.; Su Jo, M.; Jeong, S.M.; Cho, C.; Kang, Y.C.; Cho, J.S. New synthesis strategy for hollow NiO nanofibers with interstitial nanovoids prepared via electrospinning using camphene for anodes of lithium-ion batteries. J. Ind. Eng. Chem. 2019, 77, 76–82.
67. Wu, X.; Shi, Z.-Q.; Wang, C.-Y.; Jin, J. Nanostructured SiO2/C composites prepared via electrospinning and their electrochemical properties for lithium ion batteries. J. Electroanal. Chem. 2015, 746, 62–67.
68. Zhu, J.; Zhang, G.; Gu, S.; Lu, B. SnO2 nanorods on zno nanofibers: A new class of hierarchical nanostructures enabled by electrospinning as anode material for high-performance lithium-ion batteries. Electrochim. Acta 2014, 150, 308–313.
69. Zhang, J.; Li, L.; Chen, J.; He, N.; Yu, K.; Liang, C. Controllable SnO2/ hollow nanotubes prepared by electrospinning technology used as anode for lithium ion battery. J. Phys. Chem. Solids 2021, 150, 109861.
70. Chan, C.K.; Peng, H.; Liu, G.; McIlwrath, K.; Zhang, X.F.; Huggins, R.A.; Cui, Y. High-performance lithium battery anodes using silicon nanowires. Nat. Nanotechnol. 2008, 3, 31–35.
71. Lei, D.; Qu, B.; Lin, H.-T.; Wang, T. Facile approach to prepare porous GeO2/SnO2 nanofibers via a single spinneret electrospinning technique as anodes for Lithium-ion batteries. Ceram. Int. 2015, 41, 10308–10313.
72. Guo, J.; Liu, X.; Wang, H.; Sun, W.; Sun, J. Synthesis of hollow tubular reduced graphene oxide/SnO2 composites and their gas sensing properties. Mater. Lett. 2017, 209, 102–105.

73. Zhu, X.; Li, Y.; Zhang, H.; Song, L.; Zu, H.; Qin, Y.; Liu, L.; Li, Y.; Wang, F. High-performance field effect transistors based on large ratio metal (Al,Ga,Cr) doped In2O3 nanofibers. J. Alloy. Compd. 2020, 830, 154578.

74. Veeralingam, S.; Badhulika, S. Surface functionalized β-Bi2O3 nanofibers based flexible, field-effect transistor-biosensor (BioFET) for rapid, label-free detection of serotonin in biological fluids. Sens. Actuators B Chem. 2020, 321, 128540.

75. Reddy, K.C.S.; Sahatiya, P.; Santos-Sauceda, I.; Cortázar, O.; Ramírez-Bon, R. One-step fabrication of 1D p-NiO nanowire/n-Si heterojunction: Development of self-powered ultraviolet photodetector. Appl. Surf. Sci. 2020, 513, 145804.

76. Huang, X.; Zhang, M.; Qin, Y.; Chen, Y. Bead-like Co-doped ZnO with improved microwave absorption properties. Ceram. Int. 2019, 45, 7789–7796.

77. Doucey, M.A.; Carrara, S. Nanowire sensors in cancer. Trends Biotechnol. 2019, 37, 86–99.

78. Chopra, N.; Gavalas, V.G.; Hinds, B.J.; Bachas, L.G. Functional one-dimensional nanomaterials: Applications in nanoscale biosensors. Anal. Lett. 2007, 40, 2067–2096.

79. Aly, I.H.M.; Abed Alrahim Mohammed, L.; Al-Meer, S.; Elsaid, K.; Barakat, N.A.M. Preparation and characterization of wollastonite/titanium oxide nanofiber bioceramic composite as a future implant material. Ceram. Int. 2016, 42, 11525–11534.

80. Wang, X.; Gittens, R.A.; Song, R.; Tannenbaum, R.; Olivares-Navarrete, R.; Schwartz, Z.; Chen, H.; Boyan, B.D. Effects of structural properties of electrospun TiO2 nanofiber meshes on their osteogenic potential. Acta Biomater. 2012, 8, 878–885.

81. Chen, S.; Shen, L.; Huang, D.; Du, J.; Fan, X.; Wei, A.; Jia, L.; Chen, W. Facile synthesis, microstructure, formation mechanism, in vitro biocompatibility, and drug delivery property of novel dendritic TiO2 nanofibers with ultrahigh surface area. Mater. Sci. Eng. C 2020, 115, 111100.

82. Bezir, N.Ç.; Evcin, A.; Diker, R.; Özcan, B.; Klr, E.; Akarca, G.; Çetin, E.S.; Kayall, R.; Özen, M.K. Investigation of antibacterial properties of Ag doped TiO2 nanofibers prepared by electrospinning process. Open Chem. 2018, 16, 732–737.

83. Jia, L.; Huang, X.; Liang, H.; Tao, Q. Enhanced hydrophilic and antibacterial efficiencies by the synergetic effect TiO2 nanofiber and graphene oxide in cellulose acetate nanofibers. Int. J. Biol. Macromol. 2019, 132, 1039–1043.

84. Ramkumar, K.M.; Manjula, C.; Gnanakumar, G.; Kanjwal, M.A.; Sekar, T.V.; Paulmurugan, R.; Rajaguru, P. Oxidative stress-mediated cytotoxicity and apoptosis induction by TiO2 nanofibers in HeLa cells. Eur. J. Pharm. Biopharm. 2012, 81, 324–333.

85. Chen, R.; Wan, Y.; Wu, W.; Yang, C.; He, J.-H.; Cheng, J.; Jetter, R.; Ko, F.K.; Chen, Y. A lotus effect-inspired flexible and breathable membrane with hierarchical electrospinning

micro/nanofibers and ZnO nanowires. Mater. Des. 2019, 162, 246–248.

86. Thangavel, K.; Roshini, T.; Balaprakash, V.; Gowrisankar, P.; Sudha, S.; Mohan, M. Structural, morphological and antibacterial properties of ZnO nanofibers fabricated by electrospinning technique. Mater. Today Proc. 2020, 33, 2160–2166.
87. Thakur, S.; Kaur, M.; Lim, W.F.; Lal, M. Fabrication and characterization of electrospun ZnO nanofibers; antimicrobial assessment. Mater. Lett. 2020, 264.